

TOOLBOX

Quantitative chemical proteomics profiling of *de novo* protein synthesis during starvation-mediated autophagy

Jigang Wang^{a,b,i,#}, Jianbin Zhang^{a,i}, Yew-Mun Lee^b, Pin-Lang Koh^b, Shukie Ng^a, Feichao Bao^c, Qingsong Lin^b, and Han-Ming Shen^{a,d}

^aDepartment of Physiology, Yong Loo Lin School of Medicine, National University of Singapore, Singapore; ^bDepartment of Biological Sciences, National University of Singapore, Singapore; ^cDepartment of Thoracic Surgery, First Affiliated Hospital of Zhejiang University, Hangzhou, China; ^dNUS Graduate School for Integrative Sciences and Engineering, National University of Singapore, Singapore

ABSTRACT

Autophagy is an intracellular degradation mechanism in response to nutrient starvation. Via autophagy, some nonessential cellular constituents are degraded in a lysosome-dependent manner to generate biomolecules that can be utilized for maintaining the metabolic homeostasis. Although it is known that under starvation the global protein synthesis is significantly reduced mainly due to suppression of MTOR (mechanistic target of rapamycin serine/threonine kinase), emerging evidence demonstrates that *de novo* protein synthesis is involved in the autophagic process. However, characterizing these *de novo* proteins has been an issue with current techniques. Here, we developed a novel method to identify newly synthesized proteins during starvation-mediated autophagy by combining bio-orthogonal noncanonical amino acid tagging (BONCAT) and isobaric tags for relative and absolute quantitation (iTRAQTM). Using bio-orthogonal metabolic tagging, L-azidohomoalanine (AHA) was incorporated into newly synthesized proteins which were then enriched with avidin beads after a click reaction between alkyne-bearing biotin and AHA's bio-orthogonal azide moiety. The enriched proteins were subjected to iTRAQ labeling for protein identification and quantification using liquid chromatography-tandem mass spectrometry (LC-MS/MS). Via the above approach, we identified and quantified a total of 1176 proteins and among them 711 proteins were found to meet our defined criteria as *de novo* synthesized proteins during starvation-mediated autophagy. The characterized functional profiles of the 711 newly synthesized proteins by bioinformatics analysis suggest their roles in ensuring the prosurvival outcome of autophagy. Finally, we performed validation assays for some selected proteins and found that knockdown of some genes has a significant impact on starvation-induced autophagy. Thus, we think that the BONCAT-iTRAQ approach is effective in the identification of newly synthesized proteins and provides useful insights to the molecular mechanisms and biological functions of autophagy.

ARTICLE HISTORY

Received 28 September 2015
Revised 16 May 2016
Accepted 24 May 2016

KEYWORDS

AHA; autophagy; BONCAT; *de novo* protein synthesis; iTRAQ; proteomics

Introduction

Macroautophagy/autophagy is an important intracellular degradation mechanism, evolutionarily conserved in all eukaryotes.¹ The process of autophagy involves the formation of a double-membrane compartment, called the phagophore, to isolate and sequester cytoplasmic constituents such as protein aggregates and damaged organelles.^{2,3} The phagophore expands and matures into an autophagosome, which subsequently fuses with a lysosome, resulting in the formation of an autolysosome for the degradation of the sequestered materials.^{2,4} Autophagy induction involves complex regulatory mechanisms from various input factors, such as nutrient deprivation, hypoxia, and pathogen invasion.^{5,6} At the molecular level, autophagy is negatively regulated by MTOR (mechanistic target of rapamycin [serine/threonine kinase]). The inactivation of MTOR induces autophagy through the activation of the ULK1/Atg1 complex to initiate autophagosome formation.^{3,7}


Under normal conditions, autophagy occurs constitutively at basal levels, possibly reflecting its role in the degradation of long-lived proteins and the removal of damaged cellular organelles.⁸ Under stress such as starvation, enhanced autophagy flux promotes dynamic recycling of the basic biomolecules such as amino acids.⁹ These biomolecules are redirected for 2 main functions: (i) to maintain the intracellular amino acid pool for utilization in anabolic processes; and (ii) to act as substrates of the Krebs cycle for energy generation to support crucial cellular activities.¹⁰⁻¹²

Over the years, it has remained controversial as to whether the autophagic process is transcriptionally regulated, and to what extent.¹³ One important finding in recent years is that a group of nuclear transcription factors such as TP53 (tumor protein p53), STAT3 (signal transducer and activator of transcription 3), NFκB (nuclear factor of kappa light polypeptide gene enhancer in B-cells), HIF1 (hypoxia inducible factor 1), HSF1 (heat shock

CONTACT Qingsong Lin dbslinqs@nus.edu.sg Department of Biological Science, National University of Singapore, 117543, Singapore; Han-Ming Shen han-ming_shen@nuhs.edu.sg Department of Physiology, Yong Loo Lin School of Medicine, National University of Singapore, 117597, Singapore

[#]Current address: Interdisciplinary Research Group in Infectious Diseases, Singapore-MIT Alliance for Research & Technology (SMART), Singapore.

[†]These authors contributed equally to this work.

 Supplemental data for this article can be accessed on the publisher's website.

transcription factor 1), FOXO (forkhead box O) and TFEB (transcription factor EB) have been demonstrated to play important roles in autophagy regulation, mainly through transcriptional regulation, acting as either activators or repressors.^{14–19} Therefore, it is reasonable to speculate that *de novo* protein synthesis is implicated in both the basal and inducible autophagic process.

At present, little is known about the nature of proteins *de novo* synthesized during autophagy. In cells, protein expression is often adjusted to cope with the ever-changing cellular needs through the regulation of various pathways and functions. In cells undergoing autophagy, it is speculated that those newly synthesized proteins may have implications in the following 2 aspects: (i) they are directly involved in the autophagic process, such as ATG proteins; (ii) they are involved in the biological functions of autophagy, such as proteins implicated in energy metabolism, cell death, cell survival, etc. Therefore, identification and analysis of *de novo* proteins synthesized during autophagy will provide direct evidence in understanding both the regulatory mechanisms and biological functions of autophagy.

One of the main challenges in conducting a proteomic investigation on *de novo* protein synthesis during autophagy is differentiating the newly synthesized proteins from the pre-existing protein pool. Also, the abundance of the newly synthesized proteins is expected to be rather low based on the fact that during autophagy most of the protein synthesis machinery is suppressed following inhibition of MTOR.^{20,21} Thus, a robust method to identify newly synthesized proteins during autophagy is much needed.

In recent years, new techniques for the labeling and detection of *de novo* proteins have been developed. Among them, bio-orthogonal noncanonical amino acid tagging (BONCAT) has drawn wide attention. Using the simple principle of bio-orthogonal metabolic tagging, a noncanonical amino acid with a small bio-orthogonal functional group, such as the azide-bearing L-azidohomoalanine (AHA), can be incorporated into the newly synthesized proteins.^{22–24} As AHA is a methionine surrogate, it can be taken up by the cell's endogenous translational machinery naturally and efficiently.^{23,25} Importantly, the tagged *de novo* proteins can be subsequently enriched via an alkyne-bearing biotinylated tag or labeled with a fluorophore via a Cu(I)-catalyzed azide alkyne cycloaddition (CuAAC) reaction ('click chemistry').^{26,27} More recently, we have developed a novel method for quantification of autophagic protein degradation by AHA labeling,²⁸ in which the newly synthesized proteins are pulse-labeled with fluorescence and the fluorescence intensity change under autophagy is measured by flow cytometry, allowing more accurate calculation of the protein degradation rates.

Here, we report the combination of BONCAT- and iTRAQ-based quantitative proteomics methods for the specific and unbiased identification of *de novo* protein synthesis during autophagy induction by amino acid starvation. We have previously utilized iTRAQ to differentiate the specific binding proteins from the nonspecific ones during affinity enrichment.^{29,30} In the current study, via the above approach, we identified and quantified a total of 1176 proteins and among them 711 proteins were found to meet our defined criteria as *de novo* synthesized proteins during starvation-mediated autophagy. The functions of these proteins were deduced based on subsequent

bioinformatics and pathway analysis and the trends of alterations in them (promoting or inhibiting) were predicted. Functional experiments were performed to validate the role of several selected *de novo* proteins in autophagy under starvation conditions. Hence, we demonstrated the effectiveness of the BONCAT-iTRAQ approach in identifying newly synthesized proteins during autophagy, which provides novel insights in the regulatory mechanisms and biological functions of autophagy.

Results

Workflow for AHA-labeling and analysis of newly synthesized proteins in autophagy

For comprehensive profiling of the *de novo* protein synthesis during autophagy under starvation conditions, it is critical to achieve specific and efficient enrichment of these low-abundant proteins. Here, we utilized the chemical metabolic labeling method BONCAT by incorporating the azide-tagged methionine analog AHA (Fig. 1A) into the *de novo* protein synthesis process (Fig. 1B) to specifically label *de novo* proteins during autophagy. In addition, we made use of the iTRAQ-based quantitative proteomics in conjunction with BONCAT to differentiate the bona fide newly synthesized proteins from the nonspecific binding proteins during the affinity enrichment process. As shown in Fig. 1C, cells were first cultured in methionine-free medium for 30 min to deplete the natural methionine reserves. The cells were then labeled with AHA in amino acid-free medium for 2 h to induce autophagy; DMSO treatment served as a negative control. After AHA incorporation into the *de novo* proteins, the cells were harvested and lysed to react with biotin-alkyne tag and finally enriched through avidin affinity isolation in parallel. The beads were washed thoroughly, and the bound proteins were directly digested on the beads with trypsin. The resulting peptides were labeled with respective iTRAQ reagents, and pooled together for further identification and quantification via LC-MS/MS. The iTRAQ labeling enabled us to discriminate newly synthesized proteins from nonspecific and endogenously biotinylated proteins. Biological replicates of AHA- or DMSO-treated samples were included to overcome experimental variations. As shown in Fig. 1C, the AHA-labeled *de novo* proteins showed highly differential isobaric reporter intensities relative to the DMSO-treated control samples (as illustrated by the significantly higher reporter intensities of 116 and 117 than 113 and 114 shown in Fig. 1D).

Optimization of AHA-labeling of *de novo* protein synthesis during autophagy

To ensure a robust and effective AHA labeling of *de novo* proteins during autophagy, we first optimized the concentration and time of AHA-labeling. As methionine is more efficiently utilized by the endogenous methionyl-tRNA transferase, cells are incubated with methionine-free medium for 30 min prior to AHA-labeling. This aids in depleting any intracellular methionine reserves and increases the robustness of the AHA-labeling process.²³ As shown in Fig. 2A, different concentrations of

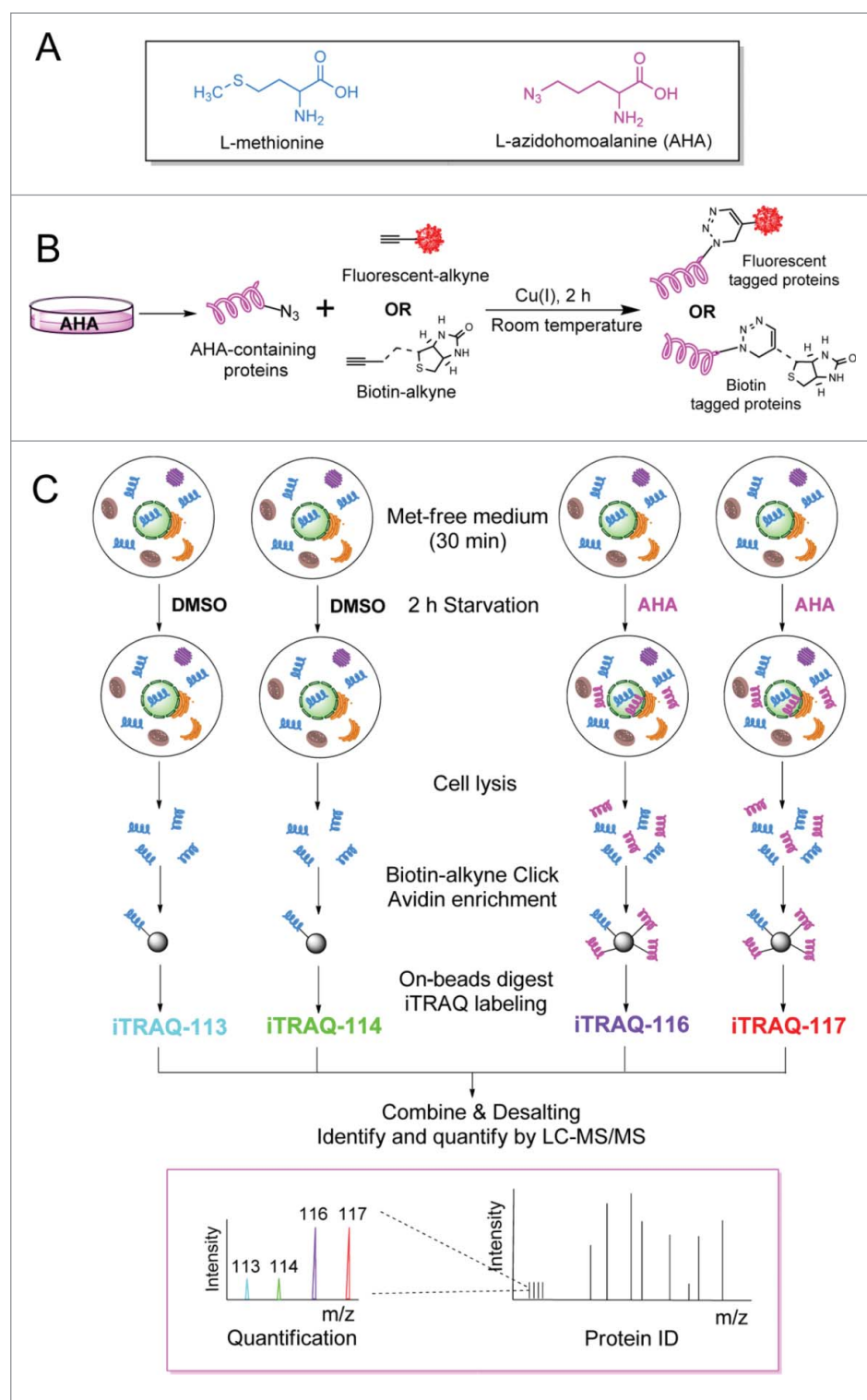


Figure 1. Workflow for AHA-labeling of *de novo* protein synthesis in autophagy. (A) Structure of L-azidohomoalanine (AHA), an analog of methionine with an azide tag. (B) AHA, which can be tagged with a fluorophore- or biotin alkyne, is used for labeling, detection and identification of newly synthesized proteins. (C) General workflow for the combined BONCAT-iTRAQ approach to detect *de novo* proteins synthesized during autophagy. HeLa cells were labeled with AHA (50 μM) or DMSO in amino acid-free medium for 2 h. The newly synthesized proteins were enriched by affinity isolation, labeled with isobaric tags and analyzed by LC-MS/MS.

AHA (50 μM to 1 mM) were tested for the optimization of AHA concentration in HeLa cells. Notably, a satisfactory fluorescent-labeling can be achieved at 50 μM of AHA and the signal intensity subsequently reached a plateau and became saturated after 100 μM . Addition of a protein synthesis inhibitor, cycloheximide (CHX), almost completely abolished the

cellular fluorescence, indicating that the labeled proteins are indeed newly synthesized.

Next, HeLa cells were incubated with AHA (50 μM) for up to 2 h in complete or amino acid-free medium. A time-dependent increase of AHA signal intensity was observed in Fig. 2B in cells cultured in complete medium. In contrast, cells cultured

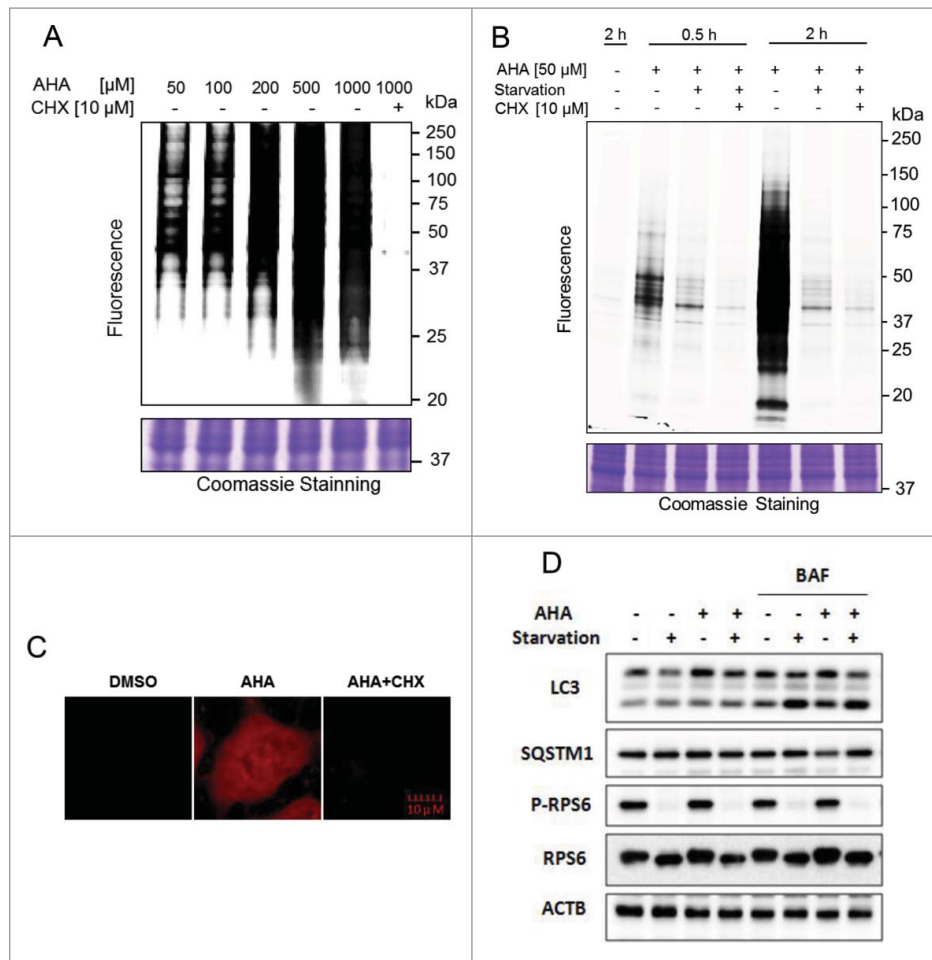


Figure 2. Optimization of AHA labeling of newly synthesized proteins during autophagy. (A) Dosage-dependent increase of AHA-labeled *de novo* proteins. HeLa cells were labeled with varying doses of AHA, ranging from $50\ \mu\text{M}$ to $1\ \text{mM}$, or in combination with CHX ($10\ \mu\text{M}$) for 30 min under normal growth conditions. Intensity of AHA-labeled proteins was observed in gel fluorescence. (B) Time-dependent increase in AHA labeling. Cells were cultured in methionine-free DMEM with 10% dialyzed fetal bovine serum and labeled with AHA ($50\ \mu\text{M}$) with or without CHX ($10\ \mu\text{M}$) for different times. Starvation was performed in amino acid-free medium. Intensity of AHA-labeled proteins was also observed in gel fluorescence. (C) HeLa cells were labeled with AHA ($50\ \mu\text{M}$) with or without CHX ($10\ \mu\text{M}$) for 2 h during autophagy induction. Intensity of AHA-labeled proteins was shown under a confocal microscope. (D) Autophagy flux level change in AHA-labeled cells. HeLa cells were labeled with AHA ($50\ \mu\text{M}$) in methionine-free medium or amino acid-free medium in the presence or absence of bafilomycin A_1 (BAF, $25\ \text{nM}$) for 2 h, and cell lysates were prepared for immunoblotting of LC3, SQSTM1, phospho (p)-RPS6 and RPS6. ACTB served as a loading control.

in amino acid-free medium showed significantly lower signal intensity. In addition, the cells were visualized under a confocal microscope. Under starvation conditions, only proteins labeled by AHA can be fluorescently detected in the cells (Fig. 2C) and addition of CHX abolished the cellular signal. No changes in cell morphology or cell viability were detected (data not shown), which is congruent with AHA being nontoxic as reported in other papers.²³ Based on the initial experiments performed, the optimal AHA-labeling condition ($50\ \mu\text{M} \times 2\ \text{h}$) was used for all subsequent experiments, unless otherwise specified.

Following optimization, it was pertinent to investigate any potential cellular effect of AHA on autophagy flux or protein metabolism that could compromise the integrity of our results. HeLa cells were treated with AHA ($50\ \mu\text{M}$) in methionine-free medium or amino acid-free medium in the presence or absence of bafilomycin A_1 (BAF) for 2 h, which inhibits the vacuolar-type H^+ -ATPase and blocks the fusion of autophagosomes with lysosomes. As shown in Fig. 2D, after adding BAF, AHA-labeling did not affect LC3-II levels under starvation

conditions, indicating that AHA-labeling did not affect the autophagy flux level. During starvation, the MTOR activity was suppressed, evidenced by the absence of phosphorylation of its downstream substrate RPS6 (Fig. 2D). Importantly, the presence of AHA in either full medium or amino acid-free medium did not affect MTOR activity (Fig. 2D).

Identification of *de novo* proteins synthesized during starvation-mediated autophagy

We used an iTRAQ quantitative proteomics approach coupled with LC-MS/MS to identify the proteins newly synthesized during autophagy induction and to distinguish them from the nonspecific binding proteins. iTRAQ reagents 113 and 114 were used to label the 2 DMSO-treated control samples, while iTRAQ reagents 116 and 117 were used to label the AHA-incorporated *de novo* proteins (Fig. 1C). To demonstrate that our biological replicates were consistent, we extracted the reporter ion peak areas and compared both biological replicates with scatter plots and regression analysis

(Fig. S1). The high R^2 values (0.987 for DMSO controls and 0.9964 for AHA labeling) suggested that our replicates were highly reproducible. ProteinPilotTM database search engine was used for the protein identification and quantification. First, only proteins with unused scores ≥ 1.3 were accepted (1176 proteins). Next, for each identified protein, 4 iTRAQ ratios of AHA-labeled versus DMSO control samples were calculated (116:113, 116:114, 117:113 and 117:114) and 1-sample t test was performed to check whether the mean log₂ ratio was truly different from 0. Only the proteins with $p \leq 0.05$ were retained (1129 proteins). To further improve the consistency of biological duplicates, only proteins with both 114:113 and 117:116 ratios falling between 0.77 and 1.3 (cutoff ratios previously determined for iTRAQ experiments to distinguish between changed and unchanged proteins) were selected (865 proteins). Proteins identified with only one peptide were then removed to further enhance the reliability of our protein identification (713 proteins). Finally, 2 proteins with mean iTRAQ ratios (116:113, 116:114, 117:113 and 117:114) less than 2 were removed from the list. As a result, 711 proteins were identified as newly synthesized proteins during autophagy induction. The flow chart of this process is summarized in Fig. S2. The mass spectrometry proteomics data have been deposited in the ProteomeXchange Consortium via the PRIDE partner repository with the dataset identifier PXD003546. The complete list of the 711 proteins is provided in Table S1.

Gene ontology analysis of the de novo synthesized proteins during autophagy

We first analyzed Gene Ontology (GO) terms for cellular components and biological processes using the Software Tool for Rapid Annotation of Proteins (developed at the Cardiovascular Proteomics Center of Boston University School of Medicine)³¹ for the 711 *de novo* proteins obtained. For the subcellular localization, 18% of the proteins were annotated as cytoplasmic proteins, 17% were identified as nuclear proteins, and 14% were classified as extracellular proteins (Fig. 3A). The remaining categories included mitochondria (6%), cytoskeleton (5%), macromolecular complexes (6%), plasma membrane (5%), and cell surface (1%), etc., whereas 16% were unclassified (Fig. 3A). Taken together, the *de novo* synthesized proteins during autophagy are broadly distributed in different compartments of the cell. Moreover, these proteins are involved in various biological processes, including cellular processes (26%), regulation (19%), metabolic processes (15%), etc. (Fig. 3B).

Multiple important biological pathways and functions implicated in autophagy

Next, we used Ingenuity Pathway Analysis (IPA) to further examine the biological pathways and cellular functions of these *de novo* synthesized proteins. The canonical pathway analysis showed that these newly synthesized proteins were highly related to EIF2S, EIF4-RPS6KB/p70S6K, MTOR and protein ubiquitination pathways, etc. (Fig. 3C). Similar analysis was performed to examine the molecular and cellular functions of these identified *de novo* proteins. As shown in

Fig. 3D, these *de novo* proteins may affect cellular growth and proliferation, cell death and survival, gene expression, DNA replication, etc. Further analysis was conducted for these top regulated functions and the results were presented as heat maps (Fig. 3E and Table S2–S5). Notably, under the functional category ‘Protein synthesis’, translation of mRNA was estimated to be reduced, as indicated by the green-colored sections. Under the category ‘Cellular growth and proliferation’, proliferation of cells and proliferation of tumor cells were predicted to be augmented, in which the red color-marked section (corresponding to an increase) was observed (Fig. 3E). For the ‘Cell death and survival’ category, cell death, necrosis and apoptosis were estimated to be reduced. In contrast, cell survival and viability were predicted to be augmented (Fig. 3E). Under the category ‘Gene expression’, translation mRNA was predicted to be downregulated, which overlapped with the findings in the category ‘Protein synthesis’. In addition, expression of mRNA was also reduced whereas DNA binding was suggested to be upregulated. The detailed information of the predicted trends of each cellular function is presented in Table S2–S11.

Validation of selected proteins involved in autophagy

The characterization of *de novo* proteins via the above-mentioned bioinformatics tools indicates that some proteins are likely to be involved in the autophagic process. Here, we performed validation assays for a group of proteins to illustrate the importance of these proteins in autophagy induction.

Recent studies suggest that mitochondria may be involved in regulating the autophagic process.^{32,33} Gomes et al.³⁴ reported that the regulation of mitochondrial morphology could determine cell fate during autophagy. Therefore, we chose 3 mitochondrial-related proteins, ATP5B (ATP synthase, H⁺ transporting, mitochondrial F1 complex, β polypeptide), HSPE1 (heat shock protein family E [Hsp10] member 1) and SLC25A3 (solute carrier family 25 member 3) for the subsequent functional validation. In addition, we also included RACK1/GNB2L1 (receptor for activated C kinase 1) and PNP (purine nucleoside phosphorylase), as they are known to be associated with autophagosome formation, based on an earlier report.³⁵ The list of the selected proteins is shown in Fig. 4A. We first evaluated the dynamic transcriptional level changes of these genes under starvation conditions by real-time PCR. As shown in Fig. 4B, in HeLa cells, there was a transient increase of these genes’ mRNA levels upon starvation (at the earlier time point of 30 min) and then a time-dependent decrease (except for ATP5B and PNP), indicating the possibility that starvation may first activate and later suppress their transcription. Such observations were generally consistent with microarray analysis in which starvation for 2 h downregulated the mRNA level of all 5 of these genes in comparison to the control cells (data not shown). Furthermore, we determined temporal patterns of these proteins under starvation conditions. As shown in the Fig. 4C, we observed an increasing trend for HSPE1 during starvation. The PNP protein level was not included due to lack of workable antibody in western blotting.

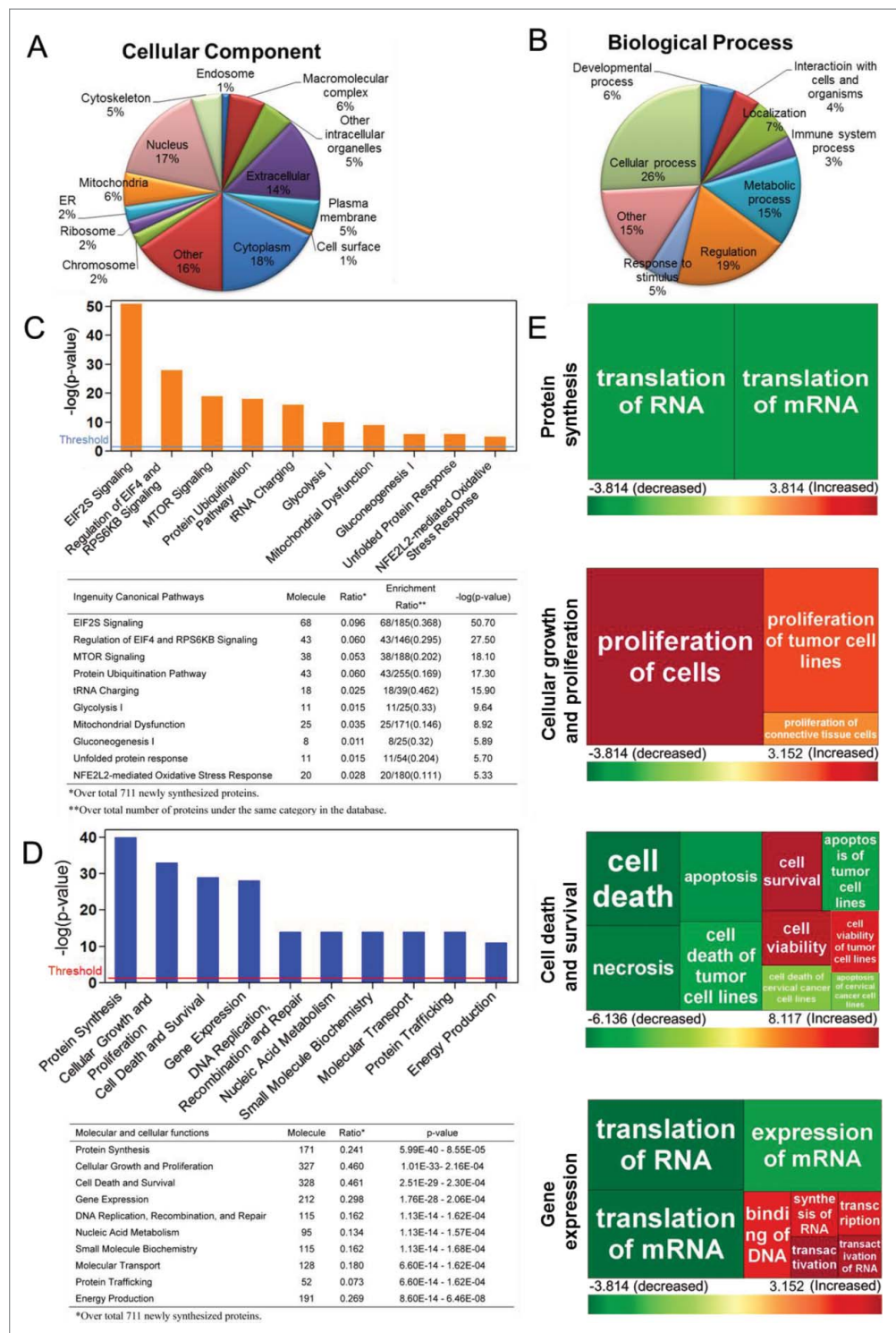


Figure 3. Gene Ontology (GO) analysis, canonical pathways, molecular and cellular functional analysis of *de novo* protein synthesis during autophagy. GO terms for cellular component (A) and biological process (B) of the *de novo* proteins analyzed based on the Software Tool for Rapid Annotation of Proteins. Proteins may be classified into multiple categories; percentages are computed as fraction of total assignments. Ingenuity Pathway Analysis (IPA) software reveals the top canonical pathways (C) and the molecular and cellular functions (D) with which the *de novo* proteins are associated. The ranking was based on the *p* values derived from the Fisher's exact test. The high-ranking categories are displayed along the x axis in a decreased order of significance. The y axis displays the $-\log(p\text{-value})$. The horizontal line denotes the cutoff threshold for significance ($p < 0.05$). The statistical data of IPA analysis are shown below the bar chart. (E) Heat maps showing the top 4 molecular and cellular functions as listed in (D), to which the newly synthesized proteins may be involved: protein synthesis, cellular growth and proliferation, cell death and survival, and gene expression. Each square represents a subcategory under the individual function indicated to the left. The size of the square is proportional to $-\log(p\text{-value})$ of the subcategory, derived from the Fisher's exact test. The color of the square corresponds to the activation z-score of the subcategory. Colors red and green indicate predicted activation and inhibition levels of individual subcategories, respectively (Tables S2–S5).

To validate the possible functional implication of these proteins in starvation-mediated autophagy, we assessed whether knockdown of these genes would affect the autophagic process.

As shown in Fig. 5A, HeLa cells were transfected with nontarget siRNA (scrambled oligonucleotides) or siRNA specifically targeting the mRNA of the 5 selected genes. The autophagic

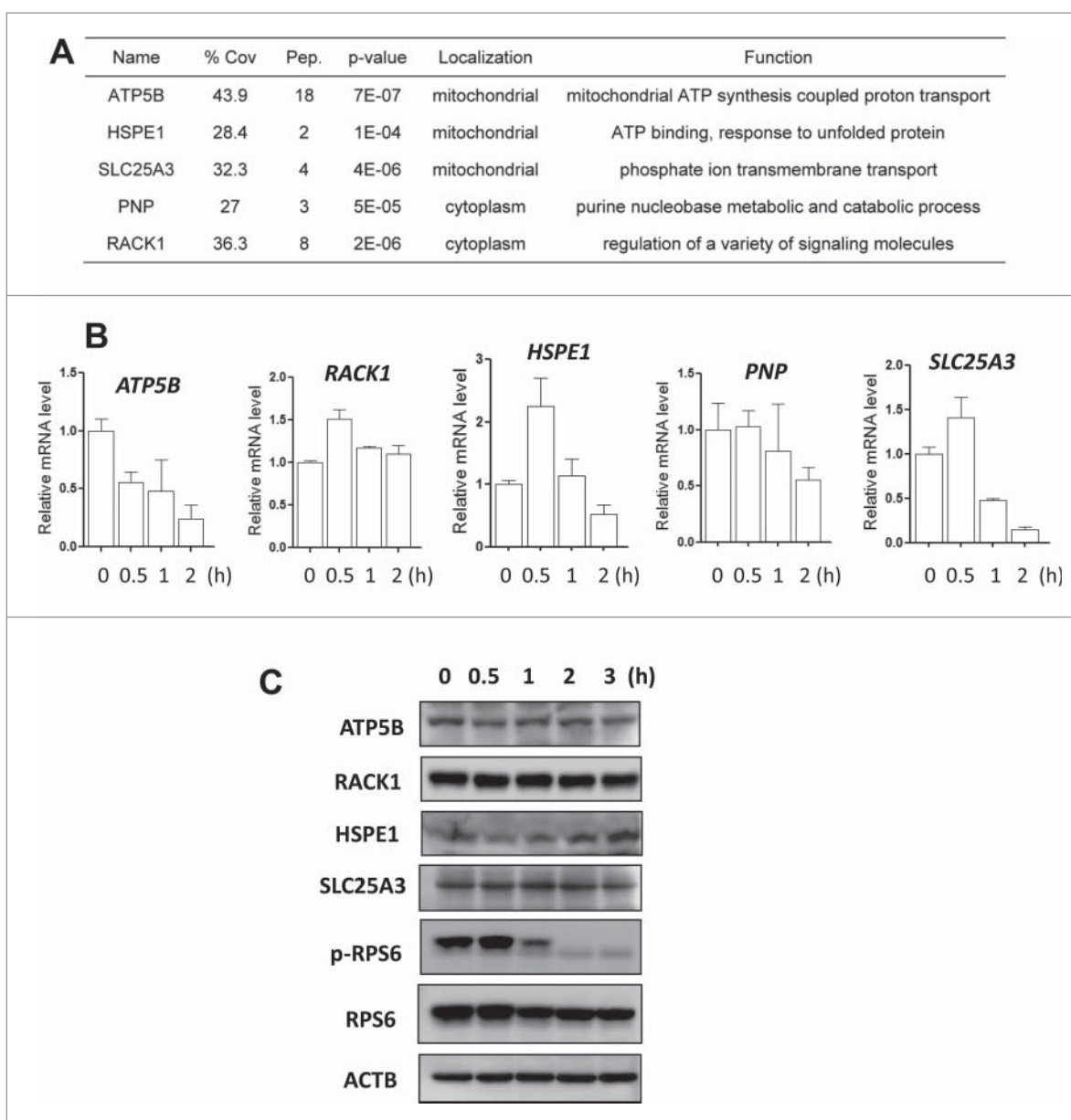


Figure 4. Transcriptional response in starvation-induced autophagy. (A) The representative newly synthesized proteins selected for the subsequent functional studies. % Cov = Coverage rate; Pep. = Numbers of peptides. (B) HeLa cells were cultured in amino acid-free medium for starvation (0.5, 1, or 2 h). Total RNA was isolated from the cells at the designated time and the mRNA levels of *ATP5B*, *RACK1*, *HSPE1*, *PNP* and *SLC25A3* were quantified by real-time PCR. *GAPDH* was used as an internal control and the fold change in mRNA levels was calculated by normalizing to *GAPDH*. (C) Dynamic changes of different proteins under starvation conditions. HeLa cells were cultured in amino acid-free medium for starvation (0.5, 1, 2 or 3 h). Cells were harvested and lysed and the protein levels of *ATP5B*, *RACK1*, *HSPE1* and *SLC25A3* were determined using western blotting. *ACTB* was used as the loading control.

flux assay (starvation in the absence or presence of BAF) showed that knockdown of *ATP5B*, *RACK1* or *SLC25A3* decreased the LC3-II level and/or increased the SQSTM1 level, reflecting a reduced autophagy flux level (Fig. 5B); while this was not seen with knockdown of *HSPE1* or *PNP*. This result indicates the positive regulatory effect of *ATP5B*, *RACK1* or *SLC25A3* in starvation-mediated autophagy. Our finding is also consistent with a very recent report³⁶ in which *RACK1* is able to promote autophagy by enhancing ATG14-BECN1-PIK3C3/VPS34-PIK3R4/VPS15 complex formation upon phosphorylation by AMPK. Therefore, our data suggest that some of these newly synthesized proteins are functionally important for starvation-induced autophagy, via mechanisms to be further elucidated.

Discussion

Autophagy is a major catabolic process induced by nutrient starvation and many other stress conditions. In recent years, there has been emerging evidence demonstrating the importance of transcriptional control of autophagy.^{37,38} For instance, several important nuclear transcriptional factors have been identified, such as TFEB, TP53, FOXOs, STAT3, etc., whereas relatively little is known about the global *de novo* protein synthesis that occurs during autophagy. Current techniques utilized in the autophagy field generally focus on improving methods of measuring rate of protein degradation and autophagic flux,^{39,40} with little effort on exploring these *de novo* proteins. On the other hand, the abundance of the newly

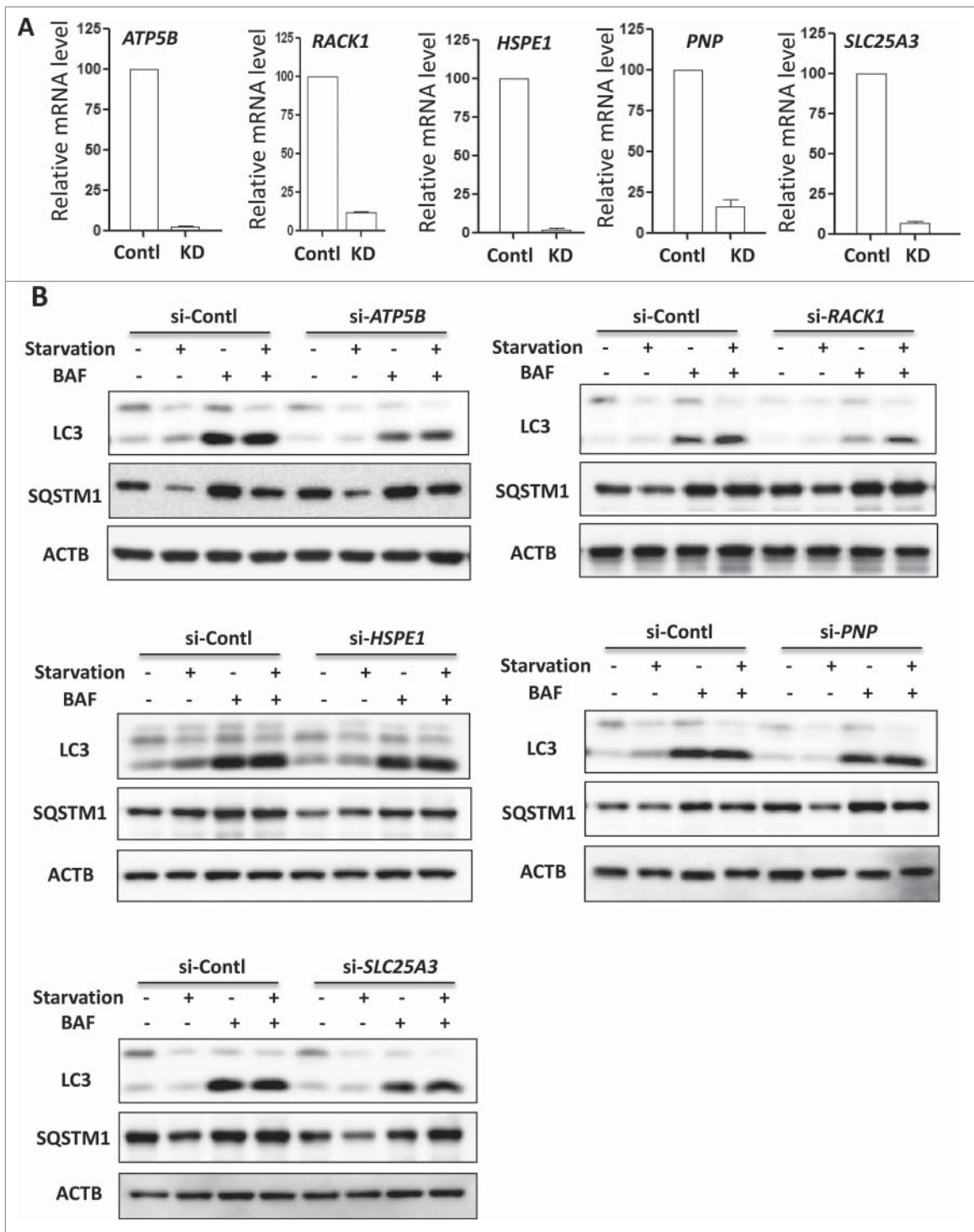


Figure 5. The involvement of newly synthesized proteins in starvation-induced autophagy. (A) HeLa cells were transiently transfected with a nonspecific siRNA or the *ATP5B*-, *RACK1*-, *HSPE1*-, *PNP*- or *SLC25A3*- targeted siRNA and treated for 2 h starvation alone or in combination with BAF (25 nM). Total RNA was isolated from HeLa cells and the mRNA levels of the above genes were quantified by real-time PCR. *GAPDH* was used as the internal control. (B) HeLa cells as described in (A) were subjected to immunoblotting of LC3 and SQSTM1 using cell lysates. ACTB served as the loading control.

synthesized proteins after autophagy induction is much lower than the pre-existing protein pool. Without specific and efficient enrichment of these proteins, it is difficult to identify them using a mass spectrometry-based proteomics approach. Although MS instruments are capable of sequencing single proteins at sub-femtomole sensitivity, the restricted dynamic range and speed of sequencing of the machine greatly limits the

effectiveness in identifying these low-abundant proteins, especially in complex mixtures.⁴¹

In this study, a novel technique was established for the identification of *de novo* protein synthesis during starvation-induced autophagy by combining a chemical metabolic labeling technology, BONCAT, with a quantitative proteomics approach (iTRAQ). The unique structure of AHA, which

consists of an azide group and a structural resemblance to methionine, allows the noncanonical amino acid to be endogenously accepted by the cell's machinery, and subsequently incorporated into *de novo* synthesized proteins.²³ More importantly, the enrichment of these newly synthesized proteins is possible via an alkyne-bearing biotinylated tag and a 'click chemistry' reaction. Although other metabolic labeling techniques such as pulsed-SILAC⁴² have been used to label and analyze newly synthesized proteins, the lack of enrichment of the labeled proteins would limit their applications in the study of autophagy, for which the protein synthesis machinery is largely suppressed. The enrichment of low-abundant proteins by BONCAT also eliminates the necessity of extensive peptide fractioning.⁴² The advantage of BONCAT in *de novo* protein enrichment and identification enables it to be applied in studying the events that occur at early or intermediate stages of biological processes, such as autophagy, which require a short period of labeling.

An iTRAQ quantitative proteomics approach was used in tandem with BONCAT to differentiate any potential background contamination from selective enrichment,^{29,30} to enhance the reliability of the results obtained. The background contamination includes the pre-existing proteins nonspecifically binding to the beads, as well as the endogenously biotinylated proteins, since streptavidin beads were used for the protein enrichment. In autophagy studies, as the protein synthesis machinery is greatly suppressed, the background contamination may be more significant due to the low abundance of the newly synthesized proteins; thus, it is highly necessary to find a way to filter them out.

While BONCAT is an attractive labeling technique to be utilized in the autophagy field, there are some technical limitations that need to be briefly addressed. First, BONCAT is limited to proteins that have at least one methionine residue, which excludes 1.02% of all known entries in the human protein database.²³ Second, during post-translational processing, it has been observed that the sole N-terminal methionine in some proteins may be removed. The proteins that undergo such processing constitute about 5.08% of all human proteins.²² Thus, a small selected group of proteins may not be successfully identified. However, the majority (at least 94%) of the mammalian proteome remains suitable as candidates for protein identification via the BONCAT approach. Hence, BONCAT can still be considered a satisfactory labeling technique for *de novo* proteins.

In addition to the technical limitations discussed above, here we would like to highlight another important issue related to this technique in our study: our method only detects the newly synthesized proteins in the course of autophagy in cells under starvation conditions, and this technique is not developed to measure or compare the protein levels between fed and starved cells. It is well known that starvation inhibits MTOR, leading to reduction of protein synthesis.^{20,21} Consistently, as shown in Fig. 2B, the levels of newly synthesized proteins were dramatically reduced in the starved cells compared to the fed cells. Therefore, it is technically difficult or infeasible to compare these 2 hugely different sets of proteins using iTRAQ

technology, mainly due to the limited dynamic range of this quantitative method. Future work is needed to make such direct comparison and to identify those proteins with increased expression in starved cells in comparison to the fed cells.

By using Gene Ontology analysis and Ingenuity Pathway Analysis, we performed some preliminary analysis of the possible biological functions of the 711 proteins identified. As shown in Fig. 3, the profiling of these proteins is generally consistent with the known regulatory mechanisms and biological function of autophagy. For instance, autophagy has been generally considered to exhibit a prosurvival effect in cells and is observed to be utilized by organisms as a survival mechanism against cellular stresses in nature.⁴³ Results from our protein analysis (Fig. 3E) indicate that some identified proteins function to promote cell proliferation, which is in concordance with the known prosurvival outcome of autophagy, suggesting that some of the newly synthesized proteins during autophagy may be crucial in ensuring the viability of the cell under extreme conditions. Other than contributing to cell survival, these proteins were also involved in the regulation of other functions, such as gene expression, metabolism of biomolecules and possibly more. This suggests that cell survival may be intricately linked with a wide array of cell functions. The regulation of various cellular functions may provide cellular signals that contribute to the prosurvival outcome of autophagy. Thus, through regulating the *de novo* proteins and their related functions, the prosurvival outcome of autophagy can be potentially modulated. This has direct implications in the field of cancer, specifically in treatments aimed at modulating autophagy activity as a possible form of cancer therapy.

Energy is an essential basic need of the cell and is required extensively in most functions. In order to ensure sufficient energy provision during periods of unfavorable conditions, autophagy is enhanced as a stress response mechanism. This allows the cell to temporarily reinstate nutrient and energy balance.¹¹ The degradation of cytoplasmic constituents and organelles during autophagy allows the production of biomolecules that can be redirected for *de novo* protein synthesis or energy generation. Current understanding of energy production during autophagy suggests that biomolecules generated from degradation are utilized as substrates for energy production. For example, amino acids can be metabolized in the tricarboxylic acid cycle for energy.⁴⁴ Also, autophagy may also prolong energy generation through ordered bulk degradation. During long-term starvation, the energy-producing mitochondria are one of the last cytoplasmic constituents to be degraded, unlike cytosolic and proteasomal proteins.⁴⁵ In our study, many of the newly synthesized proteins during autophagy were predicted to contribute to an increase in energy production and many of these proteins were located in the mitochondria. The synthesis of mitochondrial proteins, such as ATP synthase subunits and CYCS/cytochrome c, has direct implications on energy production by enhancing the efficiency of the oxidative phosphorylation pathway. Thus, this suggests that autophagy not only supports energy production through the provision of substrates but further sustains the rate of ATP production through the synthesis of these mitochondrial proteins.

Among the list of mitochondrial proteins identified, we selected several proteins for validation. Among them, the *ATP5B* gene encodes an enzyme that is a β subunit of the mitochondrial ATP synthase.⁴⁶ It is thus possible that the absence of *ATP5B* potentially impairs the ATP synthase's catalytic function in ATP synthesis. Dimerization of the enzyme may also be compromised as accessory subunits such as ATP5B aid in formation of the dimer by stabilizing the monomer-monomer interface.⁴⁷ The combined alteration is likely to hamper the efficiency of the ATP synthase in energy production.

In conclusion, in this study we successfully established a novel technique for identification of *de novo* protein synthesis during autophagy by combining a chemical metabolic labeling technology, BONCAT, with a quantitative proteomics approach (iTRAQ). As the methodology proposed here is relatively new in the field of autophagy, many studies can be further expanded and it may require the collective efforts from the entire autophagy community.

Materials and methods

Reagents and antibodies

The chemicals used in the experiments were: Click-iT AHA (L-azidohomoalanine) reagent (Invitrogen, C10289), cycloheximide (Sigma-Aldrich, C7698), tetramethylrhodamine (TAMRA) alkyne (Invitrogen, T10183), Tris (2-carboxyethyl) phosphine (TCEP; Sigma, C4706), Tris [(1-benzyl-1H-1,2,3-triazol-4-yl)methyl] amine (TBTA; Sigma-Aldrich, 678937), CuSO₄ (Sigma-Aldrich, 451657), anti-MAP1LC3/LC3 (Sigma-Aldrich, L7543), anti-SQSTM1 (Sigma-Aldrich, P0067), anti-phospho-RPS6/S6 (Ser235/236; Cell Signaling Technology, 2211), anti-RPS6 (Cell Signaling Technology, 2217), bafilomycin A₁ (Sigma-Aldrich, B1793), anti-ATP5B (Santa Cruz Biotechnology, sc-16689), anti-RACK1/GNB2L1 (Santa Cruz Biotechnology, sc-17754), anti-HSPE1 (Santa Cruz Biotechnology, sc-20958), anti-SLC25A3 (Santa Cruz Biotechnology, sc-376742) and anti-ACTB/ β -actin (Sigma-Aldrich, A5441).

Cell culture

The HeLa cell line was obtained from the American Type Culture Collection (ATCC® CCL-2™). The cell line was maintained in Dulbecco's modified Eagle's medium (DMEM; Sigma-Aldrich, D1152), supplemented with 10% fetal bovine serum (HyClone, SV30160.03). Cells were cultured in a humidified incubator at 37°C at a 5% CO₂ atmosphere.

Chemical metabolic labeling of *de novo* proteins by AHA

The HeLa cells were cultured in a 6-well plate to about 70–80% confluence and washed once with 1 × phosphate-buffered saline (PBS, 1st Base, BUF-2040-10×1L). And then the cells were subjected to L-methionine-free DMEM (Invitrogen, 21013) with 10% dialyzed fetal bovine serum (Invitrogen, 26400044) for 30 min to deplete intracellular methionine reserves. The cells were labeled by increasing concentrations of AHA (50 μ M to 1 mM) for 30 min with or without CHX in normal medium. To induce autophagy, cells were treated with

amino acid-free medium for 2 h. AHA at 50 μ M was added to metabolically label *de novo* proteins in the presence or absence of CHX (10 μ M). Finally, cells were harvested and lysed with 0.16% SDS (Sigma-Aldrich, 862010) with 1 × Halt™ Protease Inhibitor Cocktail (Pierce, 88266), 50 μ g/mL RNase (Qiagen, 19101) and 50 μ g/mL DNase (New England Biolabs, M0303S). The cell suspension was sonicated with 0.5-sec pulses for 30 sec. After centrifugation, the supernatant fraction was prepared and the protein concentration was determined using the Bradford assay before being stored at –80°C until use.

Click reaction

To detect the levels of AHA being assimilated into the proteins, a 'click' reaction between the azide-bearing AHA and an alkyne affinity tag or fluorescence dye was performed. A wide range of AHA-containing proteins with various biochemical and functional properties can be visualized using gel electrophoresis.

A cocktail of TAMRA alkyne, Tris (2-carboxyethyl) phosphine (TCEP; 1 mM, 100 × fresh stock in water), Tris [(1-benzyl-1H-1,2,3-triazol-4-yl)methyl] amine (TBTA ligand; 100 μ M, 100 × stock in DMSO), and CuSO₄ (1 mM, 100 × stock in water) was added to the cell supernatant fraction. The samples were placed on a shaker for incubation at room temperature for 2 h. Following the incubation, ice-cold acetone was added to the samples in a ratio of 4:1, with further incubation at –80°C for 30 min, to precipitate the clicked proteins. The samples were centrifuged at 14,000 × g at 4°C for 20 min before removing the supernatant fraction and allowing the pellet to air dry.

In-gel fluorescence scanning

The HeLa cells were treated, harvested, lysed and clicked accordingly. The AHA-incorporated proteins were tagged with an alkyne-bearing fluorescent dye and precipitated into a pellet. The cell pellet was dissolved in 1 × SDS loading buffer (100 μ L) and sonicated and then 25 μ L of the sample was separated via 10% SDS-PAGE. Using a Typhoon 9410 laser scanner (GE, Healthcare), the gel was imaged and analyzed using Image Quant software (GE Healthcare).

Cellular imaging of *de novo* proteins during autophagy

HeLa cells were cultured in Nunc™ Lab-Tek™ coverglass slide chambers (Thermo Fisher Scientific, 154453). To deplete intracellular methionine reserves, the cells were cultured for 30 min in L-methionine-free DMEM containing 10% dialyzed fetal bovine serum. The cells were then cultured in amino acid-free medium to induce autophagy. AHA (50 μ M) was added to metabolically label *de novo* proteins in the presence or absence of CHX (10 μ M) and the cells were cultured for up to 2 h. Subsequently, the cells were PBS-washed, followed by fixing with 4% paraformaldehyde for 15 min and then treated with 0.25% Triton™ X-100 (Sigma-Aldrich, T8787) in PBS for 15 min at room temperature to permeabilize the cell membrane. After PBS washing, the cells were soaked in PBS containing 1% BSA (Sigma-Aldrich, A8531) for 25 min for blocking, and then click chemistry was applied to fluorescently label the AHA-

containing proteins with TAMRA alkyne. The labeled cells were then examined and imaged with a confocal microscope (Olympus Fluoview FV1000).

Western blotting

Cell lysates from treated cells were separated on an SDS-PAGE gel, loaded with equal initial amounts of proteins and then transferred onto a PVDF membrane (Bio-Rad, 1620177) using a Trans-Blot Transfer System (Bio-Rad) following the manufacturer's instructions. Each blot was incubated overnight with the different primary antibodies. ACTB/ β -actin was used as the control for each experimental set to show equal loading. Prior to visualization of the blot, secondary antibodies were added following the removal of the primary antibodies. To visualize the blot, the membrane was incubated with Luminata Forte Western HRP Substrate (MERCK, WBLUF0500) and images captured using the ImageQuant LAS 500 (GE Healthcare).

Enrichment of de novo synthesized protein and on-beads digestion

Following cell treatment, HeLa cells (in a 100-mm culture dish) were processed as mentioned above for AHA labeling and click reaction. Instead of TAMRA alkyne, equal amounts of cell samples were incubated with an alkyne-biotin reagent in the 'click' reaction. The triazole formation, catalyzed by copper, between the azide group of AHA-nascent proteins and the alkyne biotin reagent allowed the newly synthesized proteins to be enriched via affinity purification with 50 μ L of streptavidin beads (Sigma-Aldrich, S1638). Initially, the cell pellet was resuspended in 0.1% SDS in PBS before 2 h-incubation with streptavidin beads at room temperature with gentle agitation. Subsequently, the beads were washed in solutions of 1% SDS, 6 M urea (Sigma, U5378) and PBS in respective order with the completion of the thrice-washing in the first solution before starting on the next. The washed beads were reconstituted in 25 mM ammonium bicarbonate (NH_4HCO_3) and reduced with incubation of 2 μ l of TCEP (100 mM stock solution) at 65°C for 60 min. The samples were further alkylated with 1 μ L of MMTS (200 mM stock solution; Pierce, 23011) in the dark at room temperature for 15 min to block cysteine residues. Trypsin (12.5 ng/ μ L; Promega, V5111) was added for overnight digestion at 37°C. The digested peptides were eluted via a filter spin column (GE, Healthcare, 27-3565-01) and stored at -20°C until further use.

Isobaric tag for relative and absolute quantification (iTRAQ) labeling

The iTRAQ labeling technique^{29,30,48} was employed to investigate the changes in the proteomic profiles upon autophagy induction, per the manufacturer's instructions with minor modifications. Briefly, the dried digested peptides were resuspended in equal amounts of dissolution buffer (0.5 M TEAB; Sigma-Aldrich, T7408). Next, the peptides were labeled with their respective isobaric tags for 2 h at room temperature before the differentially labeled peptides were pooled into a fresh tube. Strong cation exchange chromatography was performed via an iTRAQ Method

Development Kit (SCIEX, 4352160) to remove any contaminants (dissolution buffer, MMTS, SDS, calcium chloride and excess iTRAQ reagents, etc.). The samples were eluted with 5% ammonium hydroxide (NH_4OH) in 30% methanol. The eluted peptides were then desalted using a C18 Sep-Pak cartridge (Waters, WAT051910) and concentrated through lyophilization. Samples were vacuum-dried prior to reconstitution with 100 μ L of diluent (98% water, 2% acetonitrile, 0.05% formic acid).

LC-MS/MS analysis

The separation of the iTRAQ-labeled peptides was conducted via an Eksigent NanoLC-Ultra system coupled to the cHiPLC-Nanoflex system (Eksigent, Dublin, CA, USA), with a 75 μ m \times 150 mm analytical column packed with Reprosil-Pur C-18 (Eksigent, 804-00011), in Trap-Elute configuration. Five microliter of sample peptides were separated by a gradient formed by mobile phase A (2% acetonitrile (Sigma-Aldrich, 270717), 0.1% formic acid (Sigma-Aldrich, F0507)) and mobile phase B (98% acetonitrile, 2% H_2O , and 0.05% formic acid): 5–12% of mobile phase B (20 min), 12–30% of mobile phase B (90 min), 30–90% of mobile phase B (2 min), 90% of mobile phase B (5 min), 90–5% of mobile phase B (3 min), and 5% of mobile phase B (13 min), at a flow rate of 300 nl/min. The MS analysis was performed via a TripleTOF 5600 system (SCIEX) set in high-resolution mode. MS spectra were collected at the mass range of 350–1250 m/z with 250 ms accumulation time per spectrum. The further fragmentation of each MS spectrum occurred with a maximum of 20 precursors per cycle and 100 ms minimum accumulation time for each precursor across the range of 100–1800 m/z and dynamic exclusion for 15 sec. MS/MS spectra were measured in high sensitivity mode, with rolling collision energy and iTRAQ reagent collision adjustments accounted for.^{30,49}

Peptide identification and quantification

Peptide quantification and identification were performed using ProteinPilotTM Software 4.5 (SCIEX) with the Paragon algorithm (4.5.0.0, 1654). Each MS/MS spectrum was searched against SwissProt database (v2015.9) with a total of 40,406 entries. The search parameters are as listed: Cysteine alkylation with MMTS; trypsin digestion; TripleTOF 5600; biological modifications. To ensure no redundancy, the identified proteins were categorized via the ProGroup algorithm in the software. The false discovery rate for peptide identification was estimated through a decoy database search strategy. The Proteomics System Performance Evaluation Pipeline (PSPEP) feature of the ProteinPilotTM Software 4.5 was utilized to create a randomized database for this purpose.

Data analysis

Data obtained were processed and the threshold for significant protein level differences between samples was established. For protein identification, the significant total unused score cutoff of ≥ 1.3 , corresponding to $\geq 95\%$ confidence level was applied. For each identified protein, 4 iTRAQ ratios of the AHA-labeled vs. the DMSO control samples were calculated (116:113, 116:114,

117:113 and 117:114) and 1-sample *t* test was performed to check whether the mean log₂ ratio was truly different from 0. Only the proteins with $p \leq 0.05$ were retained. To determine the cutoff threshold for considering the fold changes of proteins identified from the iTRAQ study as significantly differentiated, 2 equal amounts of 6-protein mixtures (Applied Biosystems, 4352135) were trypsin-digested and labeled with the iTRAQ reagents.^{29,50-52} The standard deviation of all the ratios of the labeled peptides was computed as 0.15. Thus, with the use of a 1 ± 2 standard deviation formula, the ratio-change cutoff thresholds were set as 1.3 for upregulated proteins and reciprocally 0.77 for downregulated proteins. This strategy was adopted for our quantitative study. This cutoff was used to eliminate protein hits for which the 2 biological replicate samples showing significant changes (ratio ≥ 1.3 or ≤ 0.77) and the outliers were thus removed. To further minimize false positive proteins, any protein identified with a single peptide was dismissed to ensure the robustness of the data. Finally, a strict mean iTRAQ ratio (AHA-labeled vs. DMSO control) cutoff of 2 was adopted in the identification of the newly synthesized proteins.

Ingenuity pathway analysis

A pathway analysis of the identified *de novo* proteins was performed on the Ingenuity Pathway Analysis software (Ingenuity Systems, Redwood City, CA, USA). The proteins were mapped against the Ingenuity Pathways Knowledge base. IPA core analysis provided information on possible molecular networks and canonical pathways that the proteins regulate.

Small interfering RNA (siRNA) and transient transfection

The siRNAs targeting the *ATP5B*, *RACK1*, *HSPE1*, *PNP* and *SLC25A3* genes (Thermo Scientific, L-018615-01-0005, L-006876-00-0005, L-019649-00-0005, L-019649-00-0005, L-009579-00-0005 and L-007472-00-0005) along with scrambled RNAi oligonucleotides were transfected into HeLa cells via the DharmaFECT 4 transfection reagent (Dharmacon, T-2001-02) per the manufacturer's instructions. After 48 h, cells were treated with amino acid-free medium to induce autophagy.

Reverse transcription and quantitative real-time PCR

Using an RNeasy kit (Qiagen, 217004), RNA was extracted. Reverse transcription was conducted with 1 μ g of total RNA via a High Capacity cDNA Reverse Transcription kit (Applied Biosystems, 4368814). The mRNA expression levels were subsequently measured in triplicate using real-time PCR and SsoFast EvaGreen Supermix (Bio-Rad, 172-5201) in conjunction with the CFX96 Touch Real-time PCR Detection System (Bio-Rad). Primers for *ATP5B*, *RACK1*, *HSPE1*, *PNP* and *SLC25A3* were utilized as follows: along with *GAPDH* (glyceraldehyde-3-phosphate dehydrogenase) that served as an internal RNA loading control.

ATP5B

Forward: TCACCCAGGCTGGTTCAGA
Reverse: AGTGGCCAGGGTAGGCTGAT

RACK1

Forward: TGAGTGTGGCCTTCTCCTCT
Reverse: GCTTGCAGTTAGCCAGGTTTC

HSPE1

Forward: GGTTGAAAGGAGTGCTGCTGAA
Reverse: GAATGGGCAGCATCATGTTGAT

PNP

Forward: GTTTCCTGCCATGTCTGAT
Reverse: AGCCAAAGACTCGAAGTCCA

SLC25A3

Forward: TGCAAGCATTGAGAAAAACG
Reverse: TTCTCCTTTGCCAGCTTTGT

Statistical analysis

All western blot and image data presented are representatives from at least 3 independent experiments. The numeric data are presented as means \pm standard deviation from 3 independent experiments and analyzed using student *t* test.

Accession codes

The mass spectrometry proteomics data have been deposited in the ProteomeXchange Consortium via the PRIDE partner repository with the data set identifier PXD003546.

Abbreviations

AHA	L-azidohomoalanine
ATP5B	ATP synthase, H ⁺ transporting, mitochondrial F1 complex, β polypeptide
BAF	bafilomycin A ₁
CHX	cycloheximide
TAMRA	tetramethylrhodamine
GO	gene ontology
HSPE1	heat shock protein family E (Hsp10) member 1
iTRAQ	isobaric tags for relative and absolute quantitation
IPA	ingenuity pathway analysis
MTOR	mechanistic target of rapamycin (serine/threonine kinase)
MAP1LC3/LC3	microtubule-associated protein 1 light chain 3
PI	propidium iodide
PNP	purine nucleoside phosphorylase
RACK1/GNB2L1	receptor for activated C kinase 1
siRNA	short interfering RNA
SLC25A3	solute carrier family 25 member 3.

Disclosure of potential conflicts of interest

No potential conflicts of interest were disclosed.

Acknowledgments

We thank Dr. Henry Yang (Cancer Science Institute of Singapore, NUS) for the help in microarray analysis.

Funding

This work was supported by research grants from the National Medical Research Council Singapore (NMRC-CIRG/1346/2012 and NMRC-CIRG/

1373/2013) to HMS. Jianbin Zhang and Yew-Mun Lee are supported by NUS Research Scholarships.

References

- [1] Bauvy C, Meijer AJ, Codogno P. Assaying of autophagic protein degradation. *Methods Enzymol* 2009; 452:47-61; PMID:19200875; [http://dx.doi.org/10.1016/S0076-6879\(08\)03604-5](http://dx.doi.org/10.1016/S0076-6879(08)03604-5)
- [2] Levine B, Klionsky DJ. Development by self-digestion: molecular mechanisms and biological functions of autophagy. *Dev Cell* 2004; 6:463-77; PMID:15068787; [http://dx.doi.org/10.1016/S1534-5807\(04\)00099-1](http://dx.doi.org/10.1016/S1534-5807(04)00099-1)
- [3] Mizushima N, Komatsu M. Autophagy: renovation of cells and tissues. *Cell* 2011; 147:728-41; PMID:22078875; <http://dx.doi.org/10.1016/j.cell.2011.10.026>
- [4] Shen HM, Mizushima N. At the end of the autophagic road: an emerging understanding of lysosomal functions in autophagy. *Trends Biochem Sci* 2014; 39:61-71; PMID:24369758; <http://dx.doi.org/10.1016/j.tibs.2013.12.001>
- [5] He C, Klionsky DJ. Regulation mechanisms and signaling pathways of autophagy. *Annu Rev Genet* 2009; 43:67-93; PMID:19653858; <http://dx.doi.org/10.1146/annurev-genet-102808-114910>
- [6] Kroemer G, Marino G, Levine B. Autophagy and the integrated stress response. *Mol Cell* 2010; 40:280-93; PMID:20965422; <http://dx.doi.org/10.1016/j.molcel.2010.09.023>
- [7] Chen Y, Klionsky DJ. The regulation of autophagy - unanswered questions. *J Cell Sci* 2011; 124:161-70; PMID:21187343; <http://dx.doi.org/10.1242/jcs.064576>
- [8] Mizushima N, Klionsky DJ. Protein turnover via autophagy: implications for metabolism. *Annu Rev Nutr* 2007; 27:19-40; PMID:17311494; <http://dx.doi.org/10.1146/annurev.nutr.27.061406.093749>
- [9] Wirawan E, Vanden Berghe T, Lippens S, Agostinis P, Vandenabeele P. Autophagy: for better or for worse. *Cell Res* 2012; 22:43-61; PMID:21912435; <http://dx.doi.org/10.1038/cr.2011.152>
- [10] Kuma A, Hatano M, Matsui M, Yamamoto A, Nakaya H, Yoshimori T, Ohsumi Y, Tokuhisa T, Mizushima N. The role of autophagy during the early neonatal starvation period. *Nature* 2004; 432:1032-6; PMID:15525940; <http://dx.doi.org/10.1038/nature03029>
- [11] Lum JJ, DeBerardinis RJ, Thompson CB. Autophagy in metazoans: cell survival in the land of plenty. *Nat Rev Mol Cell Biol* 2005; 6:439-48; PMID:15928708; <http://dx.doi.org/10.1038/nrm1660>
- [12] Mizushima N. The pleiotropic role of autophagy: from protein metabolism to bactericide. *Cell Death Differ* 2005; 12 (Suppl 2):1535-41; PMID:16247501; <http://dx.doi.org/10.1038/sj.cdd.4401728>
- [13] Watanabe-Asano T, Kuma A, Mizushima N. Cycloheximide inhibits starvation-induced autophagy through mTORC1 activation. *Biochem Biophys Res Commun* 2014; 445:334-9; PMID:24525133; <http://dx.doi.org/10.1016/j.bbrc.2014.01.180>
- [14] Desai S, Liu Z, Yao J, Patel N, Chen J, Wu Y, Ahn EE, Fodstad O, Tan M. Heat shock factor 1 (HSF1) controls chemoresistance and autophagy through transcriptional regulation of autophagy-related protein 7 (ATG7). *J Biol Chem* 2013; 288:9165-76; PMID:23386620; <http://dx.doi.org/10.1074/jbc.M112.422071>
- [15] Guerriero JL, Ditsworth D, Zong WX. Non-apoptotic routes to defeat cancer. *Oncoimmunology* 2012; 1:94-6; PMID:22720222; <http://dx.doi.org/10.4161/onci.1.1.17885>
- [16] Sengupta A, Molkenin JD, Yutzey KE. FoxO transcription factors promote autophagy in cardiomyocytes. *J Biol Chem* 2009; 284:28319-31; PMID:19696026; <http://dx.doi.org/10.1074/jbc.M109.024406>
- [17] Jiang L, Sheikh MS, Huang Y. Decision Making by p53: Life versus Death. *Mol Cell Pharmacol* 2010; 2:69-77; PMID:20514355
- [18] Kreuzaler PA, Staniszewska AD, Li W, Omidvar N, Kedjouar B, Turkson J, Poli V, Flavell RA, Clarkson RW, Watson CJ. Stat3 controls lysosomal-mediated cell death in vivo. *Nat Cell Biol* 2011; 13:303-9; PMID:21336304; <http://dx.doi.org/10.1038/ncb2171>
- [19] Martinez-Outschoorn UE, Trimmer C, Lin Z, Whitaker-Menezes D, Chiavarina B, Zhou J, Wang C, Pavlides S, Martinez-Cantarín MP, Capozza F, et al. Autophagy in cancer associated fibroblasts promotes tumor cell survival: Role of hypoxia, HIF1 induction and NFkappaB activation in the tumor stromal microenvironment. *Cell Cycle* 2010; 9:3515-33; PMID:20855962; <http://dx.doi.org/10.4161/cc.9.17.12928>
- [20] Dunlop EA, Tee AR. mTOR and autophagy: a dynamic relationship governed by nutrients and energy. *Semin Cell Dev Biol* 2014; 36:121-9; PMID:25158238; <http://dx.doi.org/10.1016/j.semcdb.2014.08.006>
- [21] Russell RC, Yuan HX, Guan KL. Autophagy regulation by nutrient signaling. *Cell Res* 2014; 24:42-57; PMID:24343578; <http://dx.doi.org/10.1038/cr.2013.166>
- [22] Dieterich DC, Link AJ, Graumann J, Tirrell DA, Schuman EM. Selective identification of newly synthesized proteins in mammalian cells using bioorthogonal noncanonical amino acid tagging (BONCAT). *Proc Natl Acad Sci U S A* 2006; 103:9482-7; PMID:16769897; <http://dx.doi.org/10.1073/pnas.0601637103>
- [23] Dieterich DC, Lee JJ, Link AJ, Graumann J, Tirrell DA, Schuman EM. Labeling, detection and identification of newly synthesized proteomes with bioorthogonal non-canonical amino-acid tagging. *Nat Protoc* 2007; 2:532-40; PMID:17406607; <http://dx.doi.org/10.1038/nprot.2007.52>
- [24] Ngo JT, Tirrell DA. Noncanonical amino acids in the interrogation of cellular protein synthesis. *Acc Chem Res* 2011; 44:677-85; PMID:21815659; <http://dx.doi.org/10.1021/ar200144y>
- [25] Kiick KL, Saxon E, Tirrell DA, Bertozzi CR. Incorporation of azides into recombinant proteins for chemoselective modification by the Staudinger ligation. *Proc Natl Acad Sci U S A* 2002; 99:19-24; PMID:11752401; <http://dx.doi.org/10.1073/pnas.012583299>
- [26] Tornøe CW, Christensen C, Meldal M. Peptidotriazoles on solid phase: [1,2,3]-triazoles by regioselective copper(i)-catalyzed 1,3-dipolar cycloadditions of terminal alkynes to azides. *J Org Chem* 2002; 67:3057-64; PMID:11975567; <http://dx.doi.org/10.1021/jo011148j>
- [27] Rostovtsev VV, Green LG, Fokin VV, Sharpless KB. A stepwise Huisgen cycloaddition process: copper(I)-catalyzed regioselective "ligation" of azides and terminal alkynes. *Angew Chem Int Ed Engl* 2002; 41:2596-9; PMID:12203546; [http://dx.doi.org/10.1002/1521-3773\(20020715\)41:14%3c2596::AID-ANIE2596%3e3.0.CO;2-4](http://dx.doi.org/10.1002/1521-3773(20020715)41:14%3c2596::AID-ANIE2596%3e3.0.CO;2-4)
- [28] Zhang J, Wang J, Ng S, Lin Q, Shen HM. Development of a novel method for quantification of autophagic protein degradation by AHA labeling. *Autophagy* 2014; 10:901-12; PMID:24675368; <http://dx.doi.org/10.4161/auto.28267>
- [29] Wang J, Tan XF, Nguyen VS, Yang P, Zhou J, Gao M, Li Z, Lim TK, He Y, Ong CS, et al. A quantitative chemical proteomics approach to profile the specific cellular targets of andrographolide, a promising anticancer agent that suppresses tumor metastasis. *Mol Cell Proteomics* 2014; 13:876-86; PMID:24445406; <http://dx.doi.org/10.1074/mcp.M113.029793>
- [30] Wang J, Zhang CJ, Zhang J, He Y, Lee YM, Chen S, Lim TK, Ng S, Shen HM, Lin Q. Mapping sites of aspirin-induced acetylations in live cells by quantitative acid-cleavable activity-based protein profiling (QA-ABPP). *Sci Rep* 2015; 5:7896; PMID:25600173; <http://dx.doi.org/10.1038/srep07896>
- [31] Bhatia VN, Perlman DH, Costello CE, McComb ME. Software tool for researching annotations of proteins: open-source protein annotation software with data visualization. *Anal Chem* 2009; 81:9819-23; PMID:19839595; <http://dx.doi.org/10.1021/ac901335x>
- [32] Galluzzi L, Kepp O, Kroemer G. Mitochondrial dynamics: a strategy for avoiding autophagy. *Curr Biol* 2011; 21:R478-80; PMID:21683905; <http://dx.doi.org/10.1016/j.cub.2011.05.002>
- [33] Scherz-Shouval R, Shvets E, Fass E, Shorer H, Gil L, Elazar Z. Reactive oxygen species are essential for autophagy and specifically regulate the activity of Atg4. *EMBO J* 2007; 26:1749-60; PMID:17347651; <http://dx.doi.org/10.1038/sj.emboj.7601623>
- [34] Gomes LC, Di Benedetto G, Scorrano L. During autophagy mitochondria elongate, are spared from degradation and sustain cell viability. *Nat Cell Biol* 2011; 13:589-98; PMID:21478857; <http://dx.doi.org/10.1038/ncb2220>
- [35] Dengjel J, Hoyer-Hansen M, Nielsen MO, Eisenberg T, Harder LM, Schandorff S, Farkas T, Kirkegaard T, Becker AC, Schroeder S, et al. Identification of autophagosome-associated proteins and regulators

- by quantitative proteomic analysis and genetic screens. *Mol Cell Proteomics* 2012; 11:M111 014035; PMID:22311637; <http://dx.doi.org/10.1074/mcp.M111.014035>
- [36] Zhao Y, Wang Q, Qiu G, Zhou S, Jing Z, Wang J, Wang W, Cao J, Han K, Cheng Q, et al. RACK1 Promotes Autophagy by Enhancing the Atg14L-Beclin 1-Vps34-Vps15 Complex Formation upon Phosphorylation by AMPK. *Cell Rep* 2015; 13:1407-17; PMID:26549445; <http://dx.doi.org/10.1016/j.celrep.2015.10.011>
- [37] Lapierre LR, Kumsta C, Sandri M, Ballabio A, Hansen M. Transcriptional and epigenetic regulation of autophagy in aging. *Autophagy* 2015; 11:867-80; PMID:25836756; <http://dx.doi.org/10.1080/15548627.2015.1034410>
- [38] Fullgrabe J, Klionsky DJ, Joseph B. The return of the nucleus: transcriptional and epigenetic control of autophagy. *Nat Rev Mol Cell Biol* 2014; 15:65-74; PMID:24326622; <http://dx.doi.org/10.1038/nrm3716>
- [39] Alvarez-Castelao B, Ruiz-Rivas C, Castano JG. A critical appraisal of quantitative studies of protein degradation in the framework of cellular proteostasis. *Biochem Res Int* 2012; 2012:823597; PMID:23119163; <http://dx.doi.org/10.1155/2012/823597>
- [40] Yewdell JW, Lacsina JR, Rechsteiner MC, Nicchitta CV. Out with the old, in with the new? Comparing methods for measuring protein degradation. *Cell Biol Int* 2011; 35:457-62; PMID:21476986; <http://dx.doi.org/10.1042/CBI20110055>
- [41] de Godoy LM, Olsen JV, de Souza GA, Li G, Mortensen P, Mann M. Status of complete proteome analysis by mass spectrometry: SILAC labeled yeast as a model system. *Genome Biol* 2006; 7:R50; PMID:16784548
- [42] Eichelbaum K, Winter M, Berriel Diaz M, Herzig S, Krijgsveld J. Selective enrichment of newly synthesized proteins for quantitative secretome analysis. *Nat Biotechnol* 2012; 30:984-90; PMID:23000932; <http://dx.doi.org/10.1038/nbt.2356>
- [43] Levine B, Yuan J. Autophagy in cell death: an innocent convict? *J Clin Invest* 2005; 115:2679-88; PMID:16200202; <http://dx.doi.org/10.1172/JCI26390>
- [44] Levine B, Mizushima N, Virgin HW. Autophagy in immunity and inflammation. *Nature* 2011; 469:323-35; PMID:21248839; <http://dx.doi.org/10.1038/nature09782>
- [45] Kristensen AR, Schandorff S, Hoyer-Hansen M, Nielsen MO, Jaattela M, Dengjel J, Andersen JS. Ordered organelle degradation during starvation-induced autophagy. *Mol Cell Proteomics* 2008; 7:2419-28; PMID:18687634; <http://dx.doi.org/10.1074/mcp.M800184-MCP200>
- [46] Neckelmann N, Warner CK, Chung A, Kudoh J, Minoshima S, Fukuyama R, Maekawa M, Shimizu Y, Shimizu N, Liu JD, et al. The human ATP synthase beta subunit gene: sequence analysis, chromosome assignment, and differential expression. *Genomics* 1989; 5:829-43; PMID:2687158; [http://dx.doi.org/10.1016/0888-7543\(89\)90125-0](http://dx.doi.org/10.1016/0888-7543(89)90125-0)
- [47] Davies KM, Anselmi C, Wittig I, Faraldo-Gomez JD, Kuhlbrandt W. Structure of the yeast F1Fo-ATP synthase dimer and its role in shaping the mitochondrial cristae. *Proc Natl Acad Sci U S A* 2012; 109:13602-7; PMID:22864911; <http://dx.doi.org/10.1073/pnas.1204593109>
- [48] Ross PL, Huang YN, Marchese JN, Williamson B, Parker K, Hattan S, Khainovski N, Pillai S, Dey S, Daniels S, et al. Multiplexed protein quantitation in *Saccharomyces cerevisiae* using amine-reactive isobaric tagging reagents. *Mol Cell Proteomics* 2004; 3:1154-69; PMID:15385600; <http://dx.doi.org/10.1074/mcp.M400129-MCP200>
- [49] Wang J, Zhang CJ, Chia WN, Loh CC, Li Z, Lee YM, He Y, Yuan LX, Lim TK, Liu M, et al. Haem-activated promiscuous targeting of artemisinin in *Plasmodium falciparum*. *Nat Commun* 2015; 6:10111; PMID:26694030; <http://dx.doi.org/10.1038/ncomms10111>
- [50] Tan HT, Tan S, Lin Q, Lim TK, Hew CL, Chung MC. Quantitative and temporal proteome analysis of butyrate-treated colorectal cancer cells. *Mol Cell Proteomics* 2008; 7:1174-85; PMID:18344232; <http://dx.doi.org/10.1074/mcp.M700483-MCP200>
- [51] Higuchi S, Lin Q, Wang J, Lim TK, Joshi SB, Anand GS, Chung MC, Sheetz MP, Fujita H. Heart extracellular matrix supports cardiomyocyte differentiation of mouse embryonic stem cells. *J Biosci Bioeng* 2013; 115:320-5; PMID:23168383; <http://dx.doi.org/10.1016/j.jbiosc.2012.10.004>
- [52] Wang J, Zhang J, Zhang CJ, Wong YK, Lim TK, Hua ZC, Liu B, Tanenbaum SR, Shen HM, Lin Q. In situ Proteomic Profiling of Curcumin Targets in HCT116 Colon Cancer Cell Line. *Sci Rep* 2016; 6:22146; PMID:26915414; <http://dx.doi.org/10.1038/srep22146>